Journal of Energy Storage xxx (2016) xxx–xxx

Contents lists available at ScienceDirect

Journal of Energy Storage

journal homepage: www.elsevier.com/locate/est

The cold store for a pumped thermal energy storage system

T.R. Davenne*, S.D. Garvey, B. Cardenas, M.C. Simpson

Faculty of Engineering, The University of Nottingham, University Park, Nottingham, NG7 2RD, UK

ARTICLE INFO

Article history:
Received 15 October 2016
Received in revised form 16 February 2017
Accepted 19 March 2017
Available online xxx

Keywords:
Pumped thermal energy storage
Cold store
Wind-TP

ABSTRACT

In recent years several proposals for thermodynamic cycles involving the compression and expansion of gas and thermal storage have been put forward as effective ways of storing energy. These include the work of Desrues [1] who proposed a thermal energy storage process for large scale electric applications, Isentropic Ltd [2] who were working on a pumped thermal energy storage system and Garvey who proposed storing wind energy using a wind driven thermal pumping system known as Wind-TP [3]. All these systems require a hot and a cold store capable of storing thermal energy which can later be used to generate electricity. The efficiency and ultimately the successful adoption of pumped thermal energy storage will depend on the effectiveness of the thermal stores. In this paper we compare the performance of a packed bed and a liquid thermocline as the cold store for an off-shore Wind-TP system. Simulations are used to compare the exergetic performance of the two options leading to the conclusion that a liquid thermocline has potential to be significantly more effective than a packed bed thermocline. An addition to a liquid store involving a sliding divider separating warm and cold fluid is proposed as a way of avoiding exergy losses associated with the smearing of a thermocline front.

1. The wind driven thermal pumping cycle

In recent years several pumped thermal energy storage (PTES) systems have been put forward as efficient methods to store energy [1,2,3]. The efficiency achieved will depend on the efficiency of the constituent thermo-mechanical components. In this paper we focus on the efficiency of the thermal stores and in particular the cold store. We use the example of a wind driven thermal pumping system to evaluate the relative performance of a liquid and a packed bed cold store. The thermal pumping cycle consists of a closed circuit of working gas passing through a compressor and an expander and exchanging heat with a hot store and a cold store as shown in Fig. 1.

The cycle can operate in various modes including the following principle modes

1. Direct power transmission (no heat or coolth being transferred to stores)
2. Charging mode (heat and coolth being stored, small electrical output compared to input power)
3. Discharge mode (heat and coolth being recovered, large electrical output compared to input power)

For illustrative purposes each mode is represented in the T-S diagrams shown in Figs. 2–4 . For simplicity the compressor and expander are assumed to be isentropic and the heat exchange to and from thermal stores perfect. The working gas in the main circuit is taken to be hydrogen [3] and the pressure ratio is 25:1 with a minimum pressure of 20 bar and maximum pressure of 500 bar. The minimum temperature of the working hydrogen is 120 K and the maximum is 753 K.

An off shore wind-TP system would have a large wind turbine with rated power of at least 5 MW to be economically viable (We assume 5 MW). An energy balance around the closed gas circuit reveals that in storage mode at rated power, 5 MW of heat will be pumped into the hot store and 2 MW will be pumped out of the cold store. The aim of a wind-TP system would be to offer a wind energy storage capability on the timescale of days thus making wind power a more flexible input to the grid. We now consider how big the thermal stores would need to be to operate in charge mode at rated power for three days.

We assume an isentropic efficiency of 100% for the primary compressor and expander so the pressure and temperature ratio across these devices is related by the following

$$\frac{T_2}{T_1} = \left(\frac{P_2}{P_1}\right)^a \text{ where } a = (\gamma - 1/\gamma) \quad (1)$$

From the Steady Flow Energy Equation the compressor power and expander power can be related to the temperature change

* Corresponding author.
E-mail address: tristan.davenne@nottingham.ac.uk (T.R. Davenne).

http://dx.doi.org/10.1016/j.est.2017.03.009

Nomenclature

α	Thermal diffusivity of liquid
A	Open inlet area of thermal store
B	Exergy
D_{eff}	Effective diffusivity of a packed bed
ε	Void fraction of a packed bed
c	Thermal front velocity
C_p	Specific heat capacity
Cp_g	Specific heat capacity of gas
Cp_l	Specific heat capacity of liquid
Cp_s	Specific heat capacity of solid
γ	Ratio of specific heats
h	Heat transfer coefficient between gas and spheres in a packed bed thermocline
k	Thermal conductivity
l	Non-dimensional length scale
L	Height of thermal store
m	Mass flow
m_g	Mass flow of gas through the packed bed
m_l	Mass flow of liquid through liquid thermocline
M	Mass
M_c	Thermal mass of cold store
M_h	Thermal mass of hot store
μ	Gas viscosity
ρ_g	Density of gas
ρ_l	Density of liquid
ρ_s	Density of solid in packed bed
P	Pressure
Q	Heat flow rate
Q_b	Heat transfer rate from horizontal surfaces
Q_r	Heat transfer rate from vertical surfaces
Q_s	Heat transfer rate between gas and solid finite elements
r_p	Pressure ratio
R	Radius of the spheres within the packed bed
T	Temperature
T_c	Cold sink temperature
T_0	Reference temperature
T_g	Temperature of the gas in packed bed
T_s	Temperature of the solid in packed bed
τ	Non-dimensional time scale
t	Time
UA_r	Overall radial heat transfer coefficient
UA_b	Overall vertical heat transfer coefficient
v_s	Superficial velocity through empty packed bed
w	Insulation width
W	Mechanical power
z	Axial position in the packed bed or liquid thermocline

across them where m is the mass flow of gas through the machines and Cp is the specific heat capacity at constant pressure of the gas. Also note that in an ideal thermal pumping cycle operating in charge mode all of the power absorbed by the compressor is equivalent to the thermal power being stored in the hot store. Similarly all the power generated by the expander is equivalent to the rate of heat removal from the process gas, i.e.

$$W_{12} = Q_{23} = mCp(T_2 - T_1) \tag{2}$$

$$W_{34} = Q_{41} = mCp(T_3 - T_4) \tag{3}$$

or using Eq. (1) then we have:

$$Q_{23} = mCpT_1({r_p}^a - 1) \tag{4}$$

$$Q_{41} = mCpT_3\left(1 - \left(\frac{1}{r_p}\right)^a\right) \tag{5}$$

As the mass flow is the same through both compressor and expander and we assume that the heat exchange in the hot and cold stores are effective enough that $T_1 = T_3$ then

$$\frac{Q_{23}}{Q_{41}} = r_p^a \tag{6}$$

Now consider the required thermal mass to store energy in both hot and cold store, M_h and M_c respectively, for a finite time, δt, of operating in charge mode.

$$M_h = \frac{Q_{23}\delta t}{(T_2 - T_3)} = \frac{Q_{23}\delta t}{T_1\left(r_p^a - 1\right)} \tag{7}$$

$$M_c = \frac{Q_{41}\delta t}{(T_1 - T_4)} = \frac{Q_{41}\delta t r_p^a}{T_1\left(r_p^a - 1\right)} \tag{8}$$

Dividing to find the ratio of the required thermal mass in the hot and cold store and using equation 6 we arrive at the result that the required thermal mass of the hot store and cold store is the same

$$\frac{M_h}{M_c} = 1 \tag{9}$$

This remains the case when real isentropic efficiencies of the compressor and expander are accounted for. However it is no longer valid if the thermal stores are less than perfect. None the less it remains a good starting point for the design of a PTES system. From Eq. (7) or (8) we see that to have three days of storage at rated power the thermal stores would need to have a size of $(2\,\text{MW} \times 72\,\text{h})/(180\,\text{K}) = 2.88 \times 10^9\,\text{J/K}$. Based on the heat capacity and density of the candidate thermal storage media we assume a storage tank volume of $2525\,\text{m}^3$. For visualisation purposes this is the volume of a 5 m radius 32 m long cylinder. This is a similar size to the floats on some pilot floating wind turbine platforms and so the authors believe could realistically be housed within a wind turbine platform.

2. Exergetic efficiency of the cold store

The efficiency and ultimately the successful adoption of pumped thermal energy storage will depend on the isentropic efficiency of the compressor and expander and also the exergetic efficiency of the thermal stores. The change in exergy δB of a given mass, M, is related to the change in its thermal energy δQ and temperature T by the following expression where T_0 is a reference temperature that the mass is heated or cooled from.

$$\delta B = \left(1 - \frac{T_0}{T}\right)\delta Q \tag{10}$$

Integrating this expression as follows gives the stored exergy when the mass is changed in temperature from T_0 to T_1, i.e.

$$B_{01} = M\int_0^1 C_p\left(1 - \frac{T_0}{T}\right)dT \tag{11}$$

Please cite this article in press as: T.R. Davenne, et al., The cold store for a pumped thermal energy storage system, J. Energy Storage (2017), http://dx.doi.org/10.1016/j.est.2017.03.009

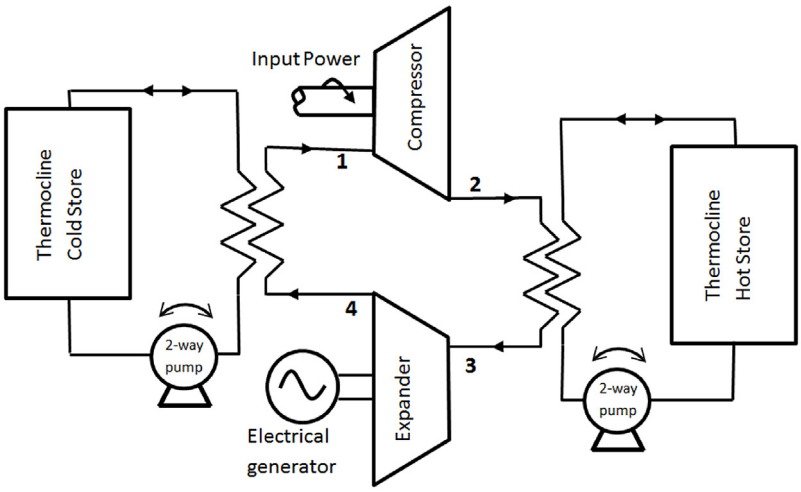

Fig. 1. Thermal pumping cycle main components.

If *Cp* is constant then

$$B_{01} = MCp(T_1 - T_0)\left(1 - \frac{T_0}{T_1 - T_0} ln\left(\frac{T_1}{T_0}\right)\right) \quad (12)$$

Exergy represents the maximum useful work possible during a process that brings the system at temperature, T_1 into equilibrium with a heat reservoir at temperature T_0. Exergy is therefore lost if for example the cold store increases in temperature towards the reference temperature. This is equally valid for the hot store loosing temperature. Fig. 5 shows the exergy loss from fully charged example cold and hot stores as they gain and loose temperature respectively. For every degree, the cold store loses more exergy than the hot store. This simple calculation highlights the need for the design of the cold store to be as effective as possible.

The main engineering challenge of the cold store is to ensure effective thermal energy storage at a temperature of 120 K. To understand this challenge we consider the following loss mechanisms that impact on effectiveness:

1. Exergy loss due to heat leak from the outside world to the thermal storage media.
2. Exergy loss when store is idle resulting from heat transfer between cold and warm material within the store.
3. Exergy destruction due to irreversible heat transfer and fluid pressure drop during charge/discharge.

Loss mechanism 1 is largely independent of the internal design of the store and is addressed by insulating the store. Assuming the tank is an insulated cylinder (Fig. 6), with insulation thickness, w, the heat transferred between the external environment temperature T_{env} and the internal temperature, T_c, can be found as follows

$$Q_r = UA_r(T_{env} - T_c) \quad (13)$$

$$\frac{1}{UA_r} = \frac{ln\left(\frac{r_2}{r_1}\right)}{2\pi Lk} + \frac{1}{2\pi r_2 Lh_r} \quad (14)$$

$$Q_b = UA_b(T_{env} - T_c) \quad (15)$$

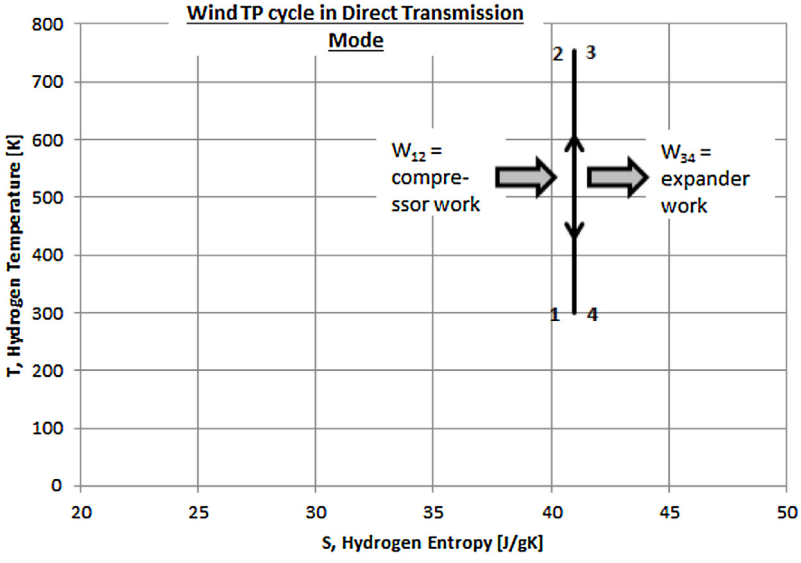

Fig. 2. T-S diagram for direct transmission.

Please cite this article in press as: T.R. Davenne, et al., The cold store for a pumped thermal energy storage system, J. Energy Storage (2017), http://dx.doi.org/10.1016/j.est.2017.03.009

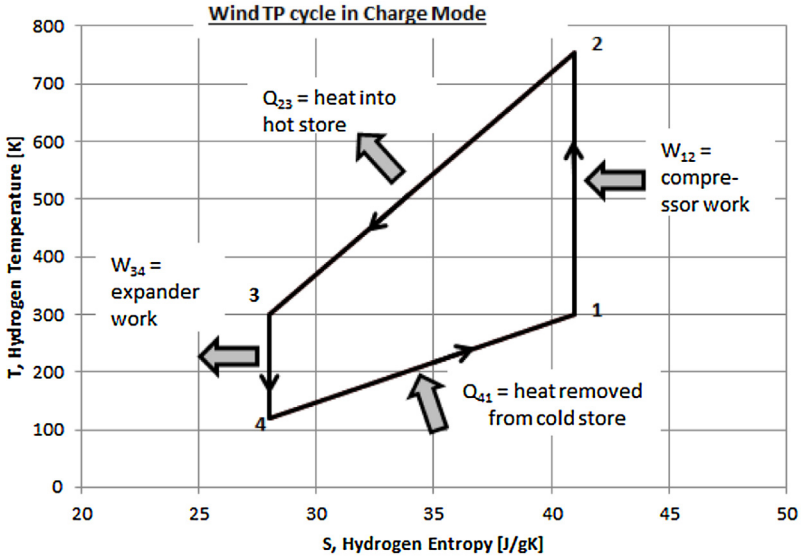

Fig. 3. T-S diagram for charge mode.

$$\frac{1}{UA_b} = \frac{w}{2k\pi {r_2}^2} + \frac{1}{2\pi {r_2}^2 h_b} \tag{16}$$

$$Q_{loss} = Q_r + Q_b \tag{17}$$

where k is the thermal conductivity of the insulation which is taken to be a typical value of 0.05 W/m K, h_r is the heat transfer coefficient on the vertical surfaces and h_b is the heat transfer coefficient on the horizontal surfaces.

Fig. 7 shows that for a 32 m long 5 m radius internal cylinder with 1 m of insulation the heat leak to the store is expected to be less than 10 kW. Calculations are done for different external heat transfer coefficients. For the case of the cold store being in still air, a typical buoyancy driven convection heat transfer coefficient of the order 1 W/m^{2}K is used. If the cold store was part of an offshore Wind-TP system it is likely to be submerged in sea water as a constituent part of a floating wind turbine platform. Simulations of heat transfer coefficients on the surface of anchored ship hulls indicate a value of the order 800 W/m^{2}K for h_r and 20 W/m^{2}K for h_b [9]. Fig. 7 indicates that it makes very little difference to the exergy loss if the store is below sea water or on ground level. This is because the overall thermal resistance is dominated by the thermal conduction through the insulation and not the surface heat transfer coefficient.

Loss mechanism 2 occurs if the store has been partially cooled and then the system goes into direct transmission mode or is turned off and the store is expected to retain the stored exergy. At the boundary between the cooled thermal storage media and the uncooled storage media heat transfer by thermal diffusion will continue to take place smearing the thermal front even though the store is idle. While no thermal energy is lost to the surroundings with this mechanism it still constitutes a loss of exergy because there is less material at the ideal storage temperature. This smearing and exergy loss can be characterised using Fick's

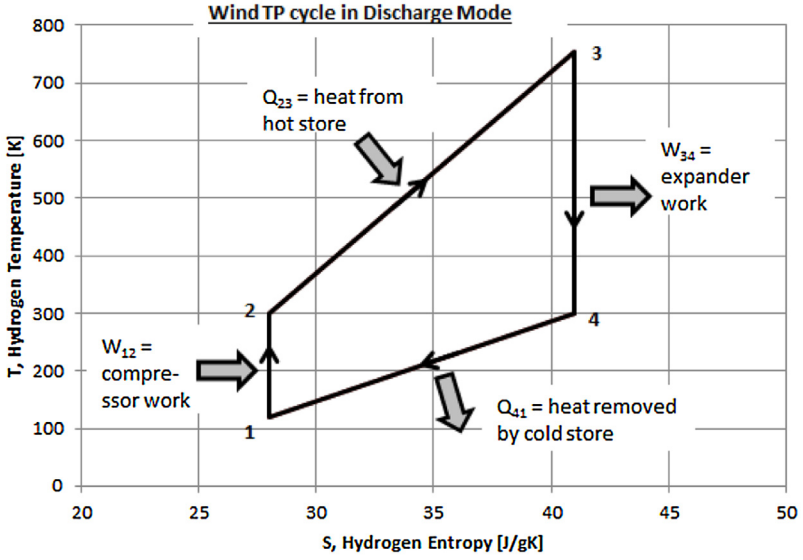

Fig. 4. T-S diagram for discharge mode.

Please cite this article in press as: T.R. Davenne, et al., The cold store for a pumped thermal energy storage system, J. Energy Storage (2017), http://dx.doi.org/10.1016/j.est.2017.03.009

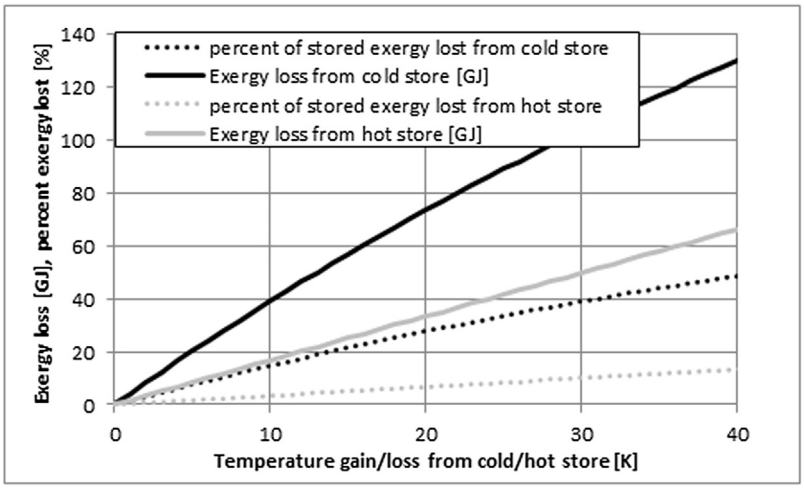

Fig. 5. Relative exergy loss from cold and hot store.

diffusion equation as follows [8]

$$\frac{\partial T}{\partial t} = \alpha \frac{\partial^2 T}{\partial z^2} \tag{18}$$

where T is temperature, α is the thermal diffusivity and z and t are position and time. We solve the equation for the following boundary conditions and initial condition which represent a square wave (i.e. a perfect abrupt thermal front) at time = 0.

$$\text{BCs} \quad \frac{\partial T}{\partial z}(z=0,t)=0 \quad and \quad \frac{\partial T}{\partial z}(z=L,t)=0 \tag{19}$$

$$\text{IC} \quad T(z,t=0)=f(z) \tag{20}$$

where

$$for \;\; 0<z<\frac{L}{2} \quad f(z)=T_c \tag{21}$$

$$for \quad \frac{L}{2}<z<L \quad f(z)=0 \tag{22}$$

Using the technique of separation of variables we arrive at the following solution

$$T(z,t)=T_c+\frac{a_0}{2}+\sum_{n=1}^{\infty} a_n cos\left(\frac{n\pi}{L}x\right)e^{\frac{-n^2\pi^2}{L^2}\alpha t} \tag{23}$$

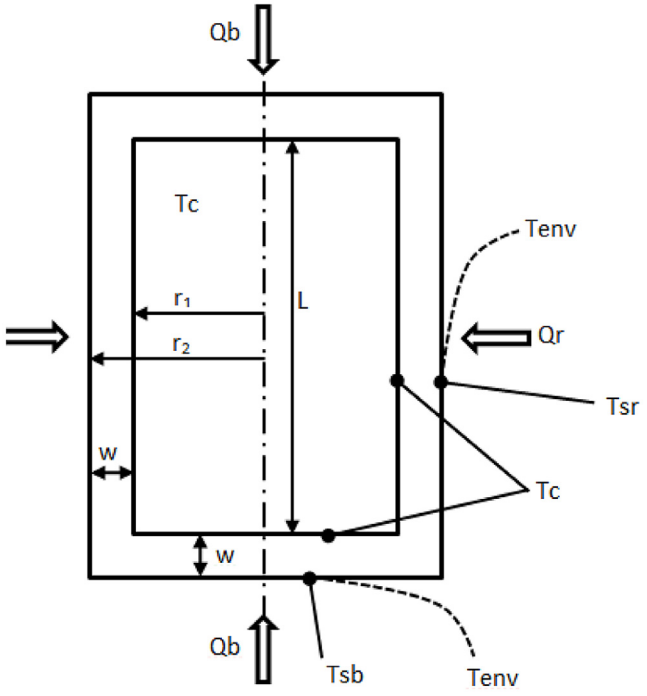

Fig. 6. Cold store heat transfer model geometry.

Please cite this article in press as: T.R. Davenne, et al., The cold store for a pumped thermal energy storage system, J. Energy Storage (2017), http://dx.doi.org/10.1016/j.est.2017.03.009

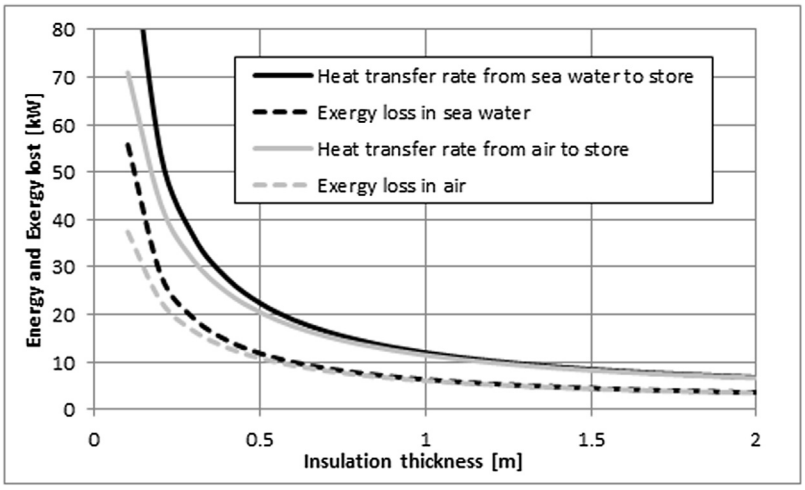

Fig. 7. Exergy loss from surface of cold store.

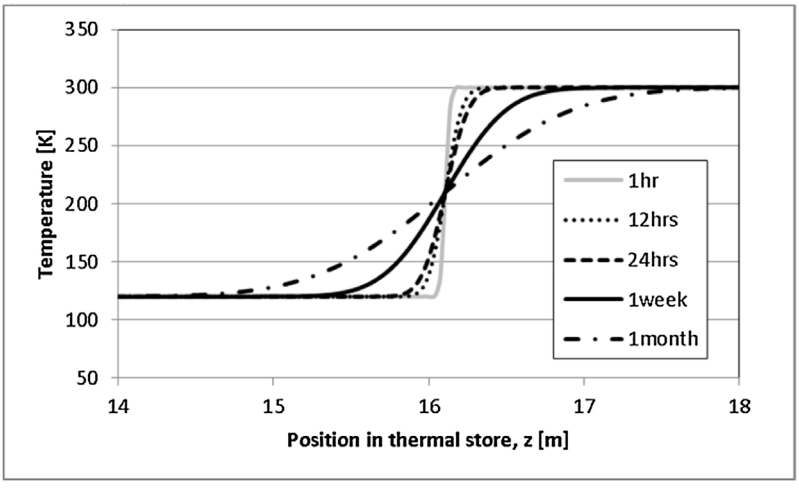

Fig. 8. Self discharge thermocline smearing from a perfect abrupt thermal front $\alpha=1\times10^{-7}\,m^2/s$ (store aspect ratio = 3).

where T_c is the cold store minimum temperature. A Fourier series expansion of the initial condition completes the solution with

$$a_0 = \frac{T_c}{2} \quad and \quad a_n = \frac{2T_c}{n\pi}\sin\left(\frac{n\pi}{2}\right) \tag{24}$$

Using this result we can plot the development of the thermocline store after it has been left partially charged (Fig. 8).

The thermal diffusivity of isopentane (the candidate fluid for a liquid store) and the effective thermal diffusivity of a nitrogen filled packed bed of concrete spheres with no flow happens to be similar at about $1\times10^{-7}\,m^2/s$. Here the effective thermal diffusivity of the packed bed is based on the effective thermal conductivity of a packed bed [10] and assumes that there is no flow which is the case when the store is idle and we are interested in self discharge. Fig. 8 shows the smearing of an abrupt thermocline in the centre of the example 32 m long 5 m radius store as a function of time. Fig. 9 shows the exergy loss associated with this smearing as a function of time. It can be seen that the loss rate falls with time and after a day is of the order 6 kW and after a week is of the order 3 kW. If the loss rate was 6 kW for a week the loss would be 2% of the total exergy stored in the half filled store.

Loss mechanism 3 is potentially much greater than the first two mechanisms considered and in contrast to the first two mechanisms considered, it does heavily depend on the internal storage media. As such we now devote our attention to predicting the losses due to irreversible heat transfer processes and fluid pressure drop with the two candidate storage media.

2.1. Packed bed thermocline

The packed bed thermocline uses a solid thermal storage media which could be closely packed spheres of concrete or equally gravel pebbles or crushed rock (depicted in Fig. 10). Piles of stacked specially moulded concrete extrusions or interlinked tiles may also be considered to ensure a regular uniform structure of the solid storage media. Heat exchange to and from the thermal storage media would be realised by either a dry gas such as nitrogen or possibly a liquid heat exchange fluid. If the heat exchange fluid is a gas the circuit would require a gas expansion chamber to account for the change in volume of the closed circuit of gas as it rises from minimum to maximum store temperature. In terms of the packed bed then granite or concrete seem to be the most economical options. Some experience of operating concrete at 113 K has been reported [5]. However it is important to note the temperature dependence of solid heat capacity at this temperature range. Quartz is a significant part of many aggregates that would be used for such a store and its heat capacity drops by more than a factor of two [6] when going from 300 K to 120 K (Fig. 17).

Please cite this article in press as: T.R. Davenne, et al., The cold store for a pumped thermal energy storage system, J. Energy Storage (2017), http://dx.doi.org/10.1016/j.est.2017.03.009

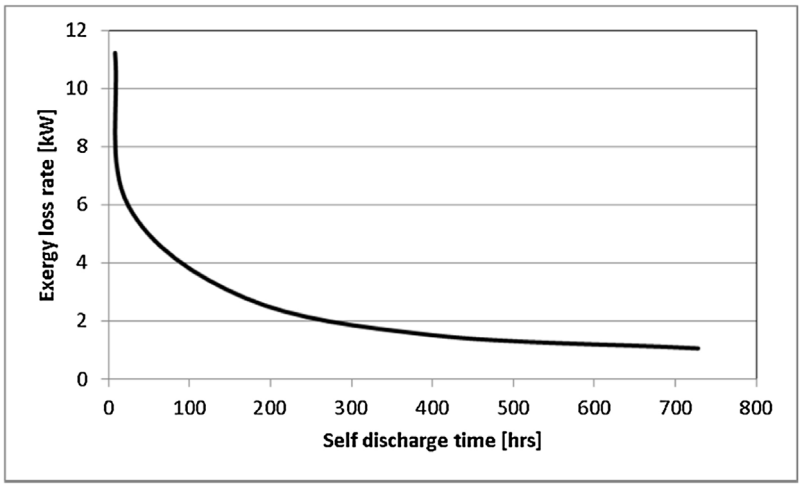

Fig. 9. Rate of Exergy loss due to self discharge (store aspect ratio = 3).

Nitrogen will remain a gas at atmospheric pressure and has a fairly constant specific heat capacity across the operating temperature range and so as long as it contains no water vapour is an obvious candidate for a packed bed heat exchange fluid.

2.2. Packed bed model

We now consider a theoretical model of a packed bed thermocline. It is first useful to write out the key equations that describe the solid and gas temperature within the packed bed to clarify the behaviour of a packed bed. Consider a one dimensional model of the packed bed (Fig. 11) with a gas and solid element at each z position along the store. In this one dimensional model we ignore peripheral losses which have been dealt with in the previous section. An energy balance of a finite element of gas and solid yields the following equation first expressed in words

Rate of change of energy within gas = Net heat flow in to element by advection – Heat transferred to the solid

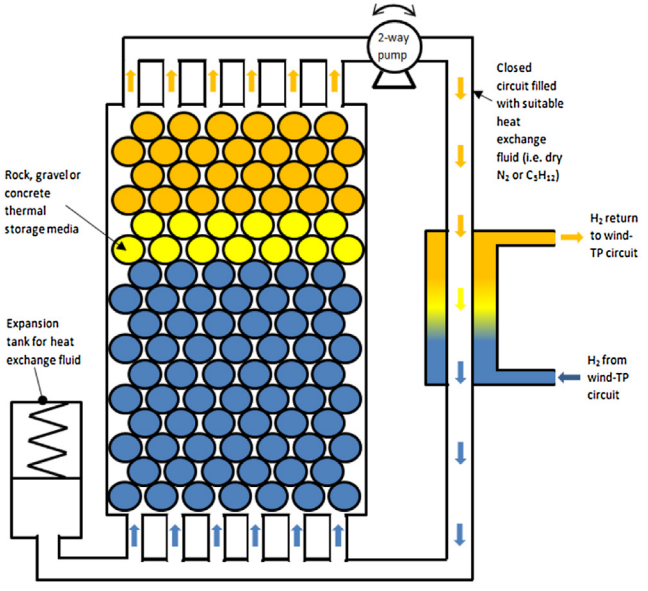

Fig. 10. Packed Bed Thermocline.

or

$$\rho_g C_{pg} A\delta z \frac{\delta T_g}{\delta t} = m_g Cp_g\left(T_g(z=\delta z) - T_g(z=2\delta z)\right) - Q_s \tag{25}$$

where the net heat flow into the gas element in the z direction is by advection only. Heat flow in the z direction by conduction is considered small and ignored here as a result of the low effective thermal conductivity of the packed bed. Note the solid elements are assumed to be thermally thin, i.e. each solid element has a uniform temperature. This is a reasonable assumption if Biot Number < 0.1 which is a desirable condition to meet for packed bed thermal stores and is the case for the parameters modeled in this paper. Heat flow to or from the solid is defined by the heat transfer rate at the surface of the packed spheres as follows

$$Q_s = hA\frac{3}{R}(1-\varepsilon)(T_g - T_s)\delta z \tag{26}$$

If any changes in energy contained within the fluid are ignored which is reasonable if the fluid has a much lower density and heat capacity than the solid, i.e.

$$\rho_g C_{pg} A\delta z \frac{\delta T_g}{\delta t} \approx 0 \tag{27}$$

then Eq. (25) becomes the following

$$m_g C_{pg}\left(T_g(z=\delta z) - T_g(z=2\delta z)\right) = \frac{3h(1-\varepsilon)(T_g - T_s)A\delta z}{R} \tag{28}$$

The rate of change of energy within the solid is also balanced by the heat transferred from gas to solid giving rise to

$$\rho_s C_{ps} A\delta z(1-\varepsilon)\frac{\delta T_s}{\delta t} = \frac{3hA(1-\varepsilon)(T_g - T_s)}{R} \tag{29}$$

In the limit $\delta z \to 0$ and $\delta t \to 0$ Eqs. (28) and (29) can be written as the following two differential equations which are known as the Schumann equations [11],

$$\frac{\partial T_g}{\partial z} = -\frac{(T_g - T_s)}{l} \tag{30}$$

and

$$\frac{\partial T_s}{\partial t} = \frac{(T_g - T_s)}{\tau} \tag{31}$$

Please cite this article in press as: T.R. Davenne, et al., The cold store for a pumped thermal energy storage system, J. Energy Storage (2017), http://dx.doi.org/10.1016/j.est.2017.03.009

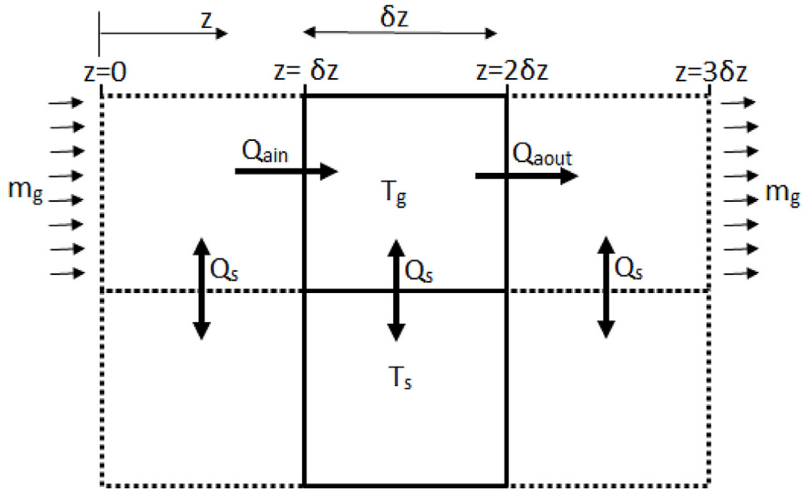

Fig. 11. One dimensional finite element model of packed bed thermal store showing gas and solid elements.

where

$$l = \frac{m_g C_{pg} R}{3hA(1-\varepsilon)} \tag{32}$$

$$\tau = \frac{\rho_s C_{ps} R}{3h} \tag{33}$$

then combining (30) and (31) to get a single equation that describes the packed bed we get to:

$$\frac{\partial T_s}{\partial t} + \frac{l}{\tau}\frac{\partial T_g}{\partial z} = 0 \tag{34}$$

Then using Eq. (30) again gives

$$T_g = T_s - (T_s - T_g) = T_s - l\frac{\partial T_g}{\partial z} \tag{35}$$

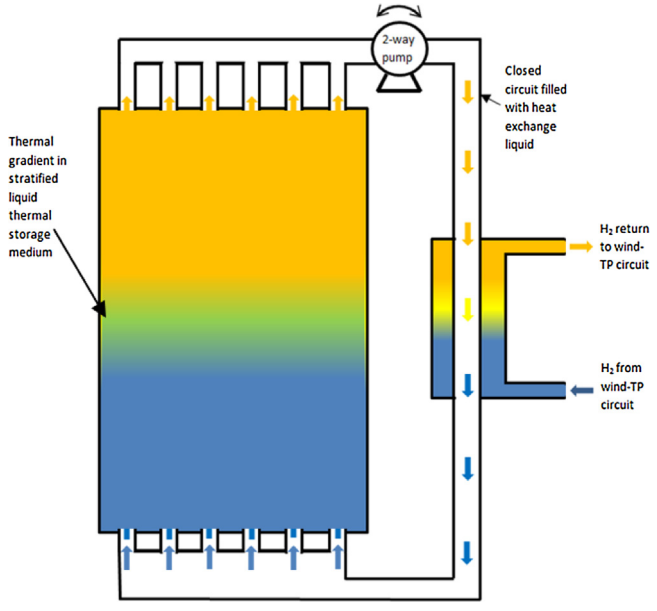

Fig. 12. Liquid thermocline.

substituting (35) into (34) gives

$$\frac{\partial T_s}{\partial t} + \frac{l}{\tau}\frac{\partial T_s}{\partial z} = \frac{l}{\tau}\frac{\partial}{\partial z} l\frac{\partial T_g}{\partial z} \tag{36}$$

if l is independent of z then we have

$$\frac{\partial T_s}{\partial t} + \frac{l}{\tau}\frac{\partial T_s}{\partial z} = \frac{l^2}{\tau}\frac{\partial^2 T_g}{\partial z^2} \tag{37}$$

We note this equation has the same form as the convection-diffusion equation where $\frac{l}{\tau}$ is the nominal speed of the thermal front and can be explicitly written as a function of the packed bed parameters

$$c = \frac{m_g C_{pg}}{A\rho_s C_{ps}(1-\varepsilon)} \tag{38}$$

and $\frac{l^2}{\tau}$ is an effective diffusivity term. The effective diffusivity of the packed bed can also be written as a function of the packed bed parameters as follows.

$$D_{eff} = \frac{{m_g}^2 {Cp_g}^2 R}{3h{A}^2(1-\varepsilon)^2 \rho_s Cp_s}\left[\frac{m^2}{s}\right] \tag{39}$$

These are useful results for quickly understanding the effect the parameters describing the packed bed have on the progression of the thermal front and ultimately the losses due to irreversible heat transfer processes. To obtain the heat transfer coefficient we use published Nusselt number correlations. At low Reynolds number which is the regime these type of packed bed stores work in, the heat transfer coefficient is well approximated by the following expression

$$Nu = \frac{2hR}{k} = 0.07Re = 0.14\frac{\rho_g UR}{\mu} \tag{40}$$

It is a reasonable fit to the data of Kunii et al. and Cybulski et al. in the Reynolds number range 0.1 to 100 [14]. Using this expression also indicates that h is independent of sphere diameter at low Reynolds number. Other Nusselt number correlations such as that of Achenbach may be suitable for higher Reynolds number flows. To solve the Schumann equations describing the packed bed we have employed a semi-implicit method as described by White et al. [12,13,15] (Appendix A). By way of validation we also employ an explicit method which unlike the Schumann equations accounts for axial conduction and energy change in the heat transfer fluid (described in Appendix B). If axial conductivity is set to zero in the explicit method perfect agreement with the semi-implicit method

Please cite this article in press as: T.R. Davenne, et al., The cold store for a pumped thermal energy storage system, J. Energy Storage (2017), http://dx.doi.org/10.1016/j.est.2017.03.009

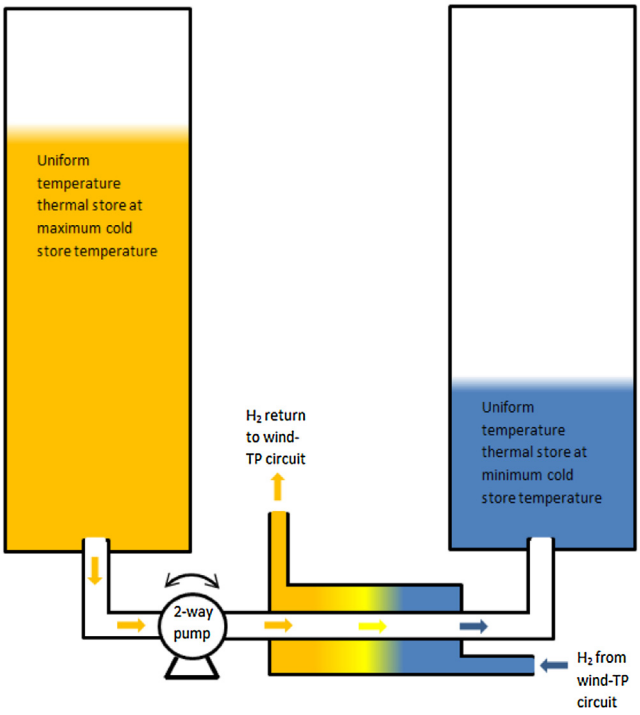

Fig. 13. Twin tank liquid thermal store.

is achieved. On the whole axial conduction was found to have a small effect on bed performance but does become noticeable at low packed bed aspect ratios i.e. tending towards unity.

2.3. Liquid thermocline

The liquid thermocline consists of a tank full of liquid with a stratified thermal gradient (Fig. 12). In this case the thermal storage media can also act as the heat exchange fluid transferring heat directly with the Wind-TP thermal pumping circuit. However it is important to avoid perturbing the delicate thermocline [4] by adding turbulence or non-uniform momentum at the inlet as this can be a source of significant exergy destruction. Fig. 13 shows a twin tank system with each tank having its own uniform temperature, the thermal storage media flows from one tank to the other and is heated or cooled by the working gas as it passes between the tanks. One tank is at the minimum cold store temperature and the other is at the reference temperature. This avoids the loss associated with a thermocline, however it does add extra cost as it requires double the tank volume for a given thermal mass of storage media.

There are a limited number of liquids suitable for a cold store, the main criteria being that they remain a liquid across the desired operating temperature range of the cold store. Results of a survey of fluids from the NIST database revealed isopentane as a candidate with a melting temperature of 112 K and boiling temp of 301 K at atmospheric pressure (Fig. 14). Propane and ethanol have also been considered however at atmospheric pressure they would not cover the temperature range individually. One option would be to pressurise the propane to over 10 bar however this clearly increases the cost of the tank. The boiling temperature of propane goes up from 230 K at atmospheric pressure to 300 K at 10 bar

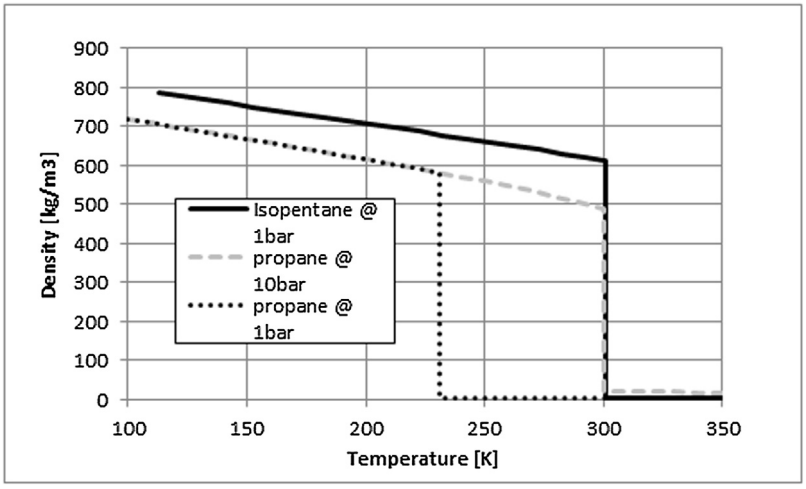

Fig. 14. Density of isopentane C_5H_{12} and propane C_3H_8.

Please cite this article in press as: T.R. Davenne, et al., The cold store for a pumped thermal energy storage system, J. Energy Storage (2017), http://dx.doi.org/10.1016/j.est.2017.03.009

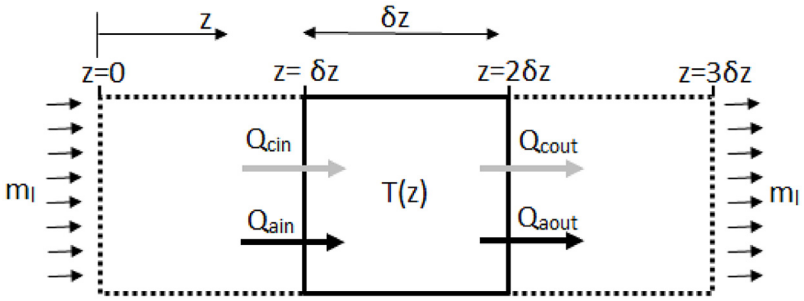

Fig. 15. One dimensional finite element model of liquid thermocline model.

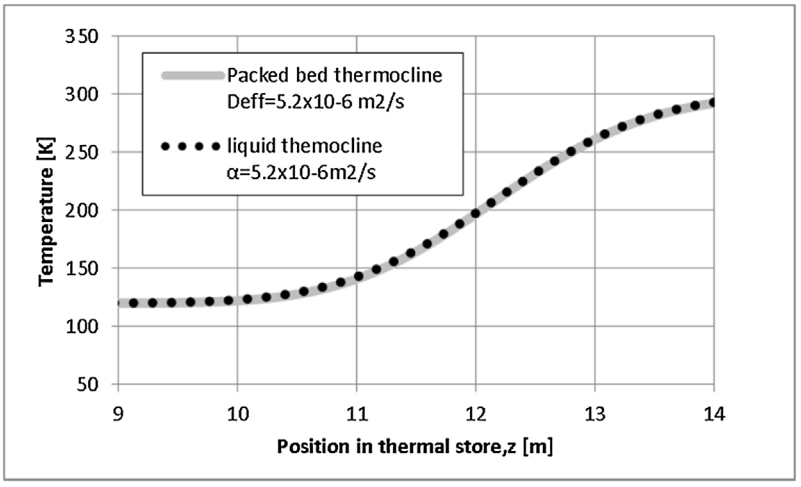

Fig. 16. Thermocline shape following a given charge time in a packed bed and a liquid thermocline with equivalent thermal diffusivities and thermal front velocities.

(Fig. 14). Alternatively to avoid the need for pressurisation one could envisage a two tier store where the hot part is served by ethanol and the cold part by propane with a propane ethanol heat exchanger between the two tiers. This would clearly involve extra cost and complexity and hence we favour isopentane for a liquid cold store.

2.4. Liquid thermocline model

Consider a one dimensional model of a liquid thermocline as shown in Fig. 15. An energy balance on a finite element of the liquid thermocline gives

Rate of change of energy within liquid element = Net heat flow in to element by advection + Net heat flow into element by conduction

This can be expressed as

$$\rho_l C_{pl} A \delta z \frac{\delta T}{\delta t} = m_l C p_l (T(z=\delta z) - T(z=2\delta z)) + \frac{k_l A}{\delta z}(T(z = 0.5\delta z) - 2T(z=1.5\delta z) + T(z=2.5\delta z)) \quad (41)$$

As $\delta z \to 0$ and $\delta t \to 0$ then Eq. (41) can be written as the convection-diffusion equation

$$\frac{\partial T}{\partial t} = \alpha \frac{\partial^2 T}{\partial z^2} + c\frac{\partial T}{\partial z} \quad (42)$$

where T is temperature, $\alpha = \frac{k_l}{Cp_l \rho_l}$, is the thermal diffusivity and $c = \frac{m_l}{\rho_l A}$, represents the thermal front velocity. The position of the thermal front simply depends on the amount of fluid that is pumped in or out of the store and the shape of the thermal front depends on the thermal diffusivity. The design goal of a liquid thermocline is to achieve laminar perfectly stratified flow. In this case α is just a function of the liquid fundamental properties. If the thermocline is perturbed then this may be represented by using a turbulent diffusivity. We apply a simple explicit numerical method to solve this equation as detailed in Appendix C.

It is worth noting at this point the similarity between the equations describing the packed bed and the liquid thermocline i.e. Eqs. (37) and (42) respectively. Infact if the thermal diffusivity of the liquid is set to equal the effective diffusivity of the packed bed then equivalent thermocline shapes can be obtained (Fig. 16). This works because the difference between solid and gas temperature profiles is often very small so Eq. (37) behaves like the convection diffusion equation. This indicates that the diffusivity of a store, whether it be the effective diffusivity of a packed bed or the diffusivity of a liquid thermocline, is a useful metric for gauging the effectiveness of a thermal store.

3. Results

We now present a comparison of results obtained from the packed bed and liquid thermocline models. For the liquid thermocline the available volume ($2525\,m^3$) is filled with isopentane providing the required thermal mass of 2.88×10^9 J/K based on a nominal heat capacity and density of 1900 J/kgK and 700 kg/m^3 respectively. The packed bed model is based on concrete spheres with nitrogen gas as the heat transfer fluid. The thermal

Table 1
Example charge discharge cycle applied at rated power.

Time	Direction	Inlet temperature
0–28 h	Charge	120
28–48 h	Discharge	300
48–68 h	Charge	120
68–88 h	Discharge	300
88–108 h	Charge	120
108–128 h	Discharge	300
128–148 h	Charge	120
148–168 h	Discharge	300
168–188 h	Charge	120

mass requirement of 2.88×10^9 J/K is achieved by filling the available volume with concrete (density 2400 kg/m^3 and specific heat capacity 769 J/kgK) to a realistically achievable solid fraction of 0.55.

An example operational cycle is used to evaluate the thermal performance of both stores. Table 1 shows the charge discharge duty used.

Fig. 17 shows the volumetric heat capacity of isopentane relative to that of quartz. Maintaining heat capacity at low temperature is clearly good from the point of view of minimizing the required volume of a cold store. The authors wish to note that the specific heat capacity and volumetric heat capacity of isopentane does not fall away as temperature reduces in the same manor as a solid thermal medium.

The reduction in heat capacity of the solid storage media at low temperature has a significant effect on the propagating thermocline. The cold part of the front travels faster than the hot part of the front which can be seen from examination of Eq. (38). This means that during charging the front becomes steeper than it would be with constant heat capacity and during discharging it smears out more quickly. Fig. 18 shows the symmetric shape of the packed bed thermal front if we assume the specific heat capacity remains at the ambient temperature level as compared to the realistic case of a temperature dependant heat capacity. The steeper front will cause increased thermal diffusion due to the higher temperature gradient, however during discharge the front becomes much less steep and so diffusion is reduced during discharging. The overall effect on diffusion during a realistic duty cycle is small. However Fig. 18 reveals how the reduction in heat capacity of the solid will mean that outlet temperature during discharge will be compromised much sooner as a result of reduced heat capacity at low temperature. It also highlights the fact that a drop in heat capacity at low temperature will increase the required size of the store for a given exergy storage capacity.

The size of the packed bed spheres has a significant effect on the smearing of the thermal front. Fig. 19 shows thermal fronts after 28 h of charging at nominal power with two different size spheres. The larger spheres have increased diffusion as is expected from examination of Eq. (39). It can also be seen that the gas temperature in the packed bed leads the solid temperature (Fig. 19). The two thermal fronts are almost overlaid for fairly small sphere sizes. The lead is more noticeable with larger spheres due to the lower heat transfer area that results from larger spheres.

Fig. 20 shows the temperature of 5 mm radius solid spheres in the packed bed thermocline at several points in the example cycle. The temperature dependent effective diffusivity is of the order 5×10^{-6} m^2/s. The degradation of the thermal front after successive charge discharge periods can be seen. By contrast the thermal diffusivity of isopentane is taken as 1×10^{-7} m^2/s and is assumed to be a constant across the temperature range. Fig. 21 shows the shape of the thermal front after the same points in the charge discharge cycle. This comparative analysis serves to show how potentially effective a liquid thermocline can be if it is perfectly stratified. By comparison it is clear from Fig. 20 that the packed bed experiences significantly more dissipation of the thermal front.

In order to quantify the difference in performance of the packed bed and liquid thermoclines the exergy loss accrued after completion of the example duty cycle is calculated. Both stores are being charged and discharged with mass flows corresponding to the nominal thermal pumping rate of 2 MW. We integrate Eq. (11) to determine the exergy stored in each finite mass of the thermal store. If heat capacity is a function of temperature,

i.e. $Cp_s = AT + B$ then the integral becomes

$$B_{01} = m\left(\frac{A}{2}\left(T_1^{\,2} - T_0^{\,2}\right) + (B - AT_0)(T_1 - T_0) - BT_0 ln\left(\frac{T_1}{T_0}\right)\right) \quad (43)$$

We can do this for both the liquid and packed bed thermocline and find the exergy contained within the stores at any moment during the charge discharge cycle. The cumulative exergy flow in and out of the store is also obtained during the computation. We can then define an exergy loss as follows

$$exergy\ \ lost = net\ \ exergy\ flowed\ in - exergy\ in\ \ store \quad (44)$$

For the packed bed store the pressure difference required to pump the nitrogen through the packed bed must also be

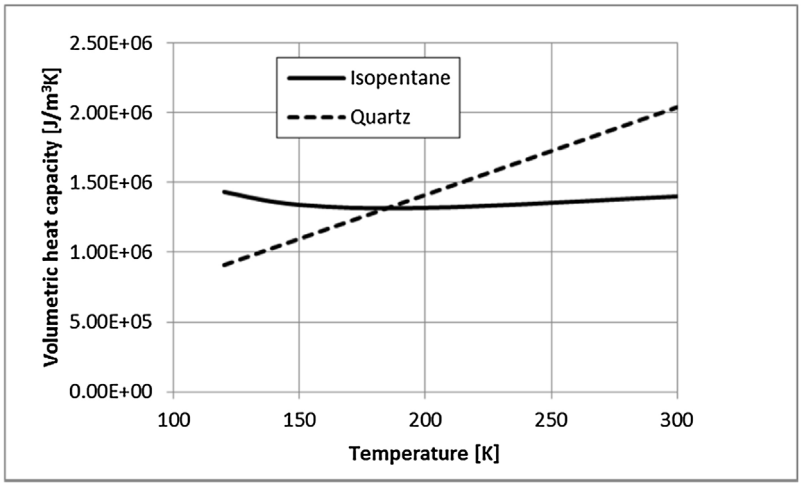

Fig. 17. Volumetric heat capacity of C_5H_{12}.

Please cite this article in press as: T.R. Davenne, et al., The cold store for a pumped thermal energy storage system, J. Energy Storage (2017), http://dx.doi.org/10.1016/j.est.2017.03.009

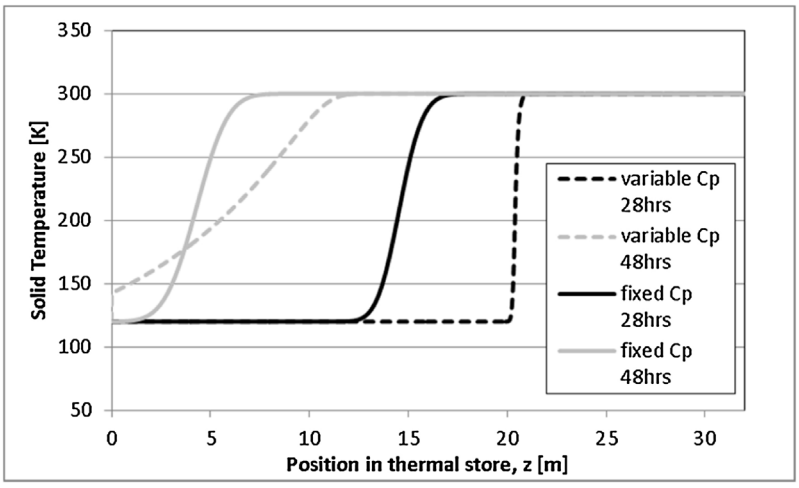

Fig. 18. Effect of specific heat capacity of the solid reducing with temperature.

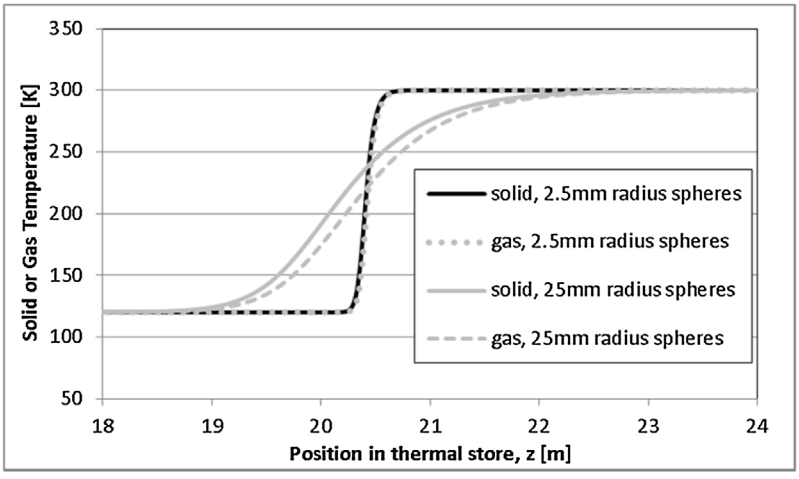

Fig. 19. Gas and Solid temperature in thermocline after 28 h of charging at nominal power for two different sphere radii.

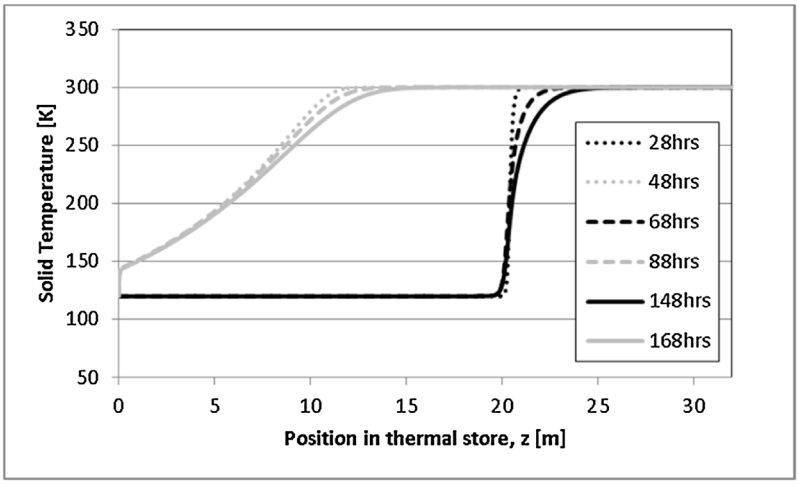

Fig. 20. Progression of thermal front in packed bed store following charge discharge cycle shown in Table 1 with nominal 2 MW of heat being pumping out of the store during charging (11.1 kg/s of nitrogen at 120 K).

Please cite this article in press as: T.R. Davenne, et al., The cold store for a pumped thermal energy storage system, J. Energy Storage (2017), http://dx.doi.org/10.1016/j.est.2017.03.009

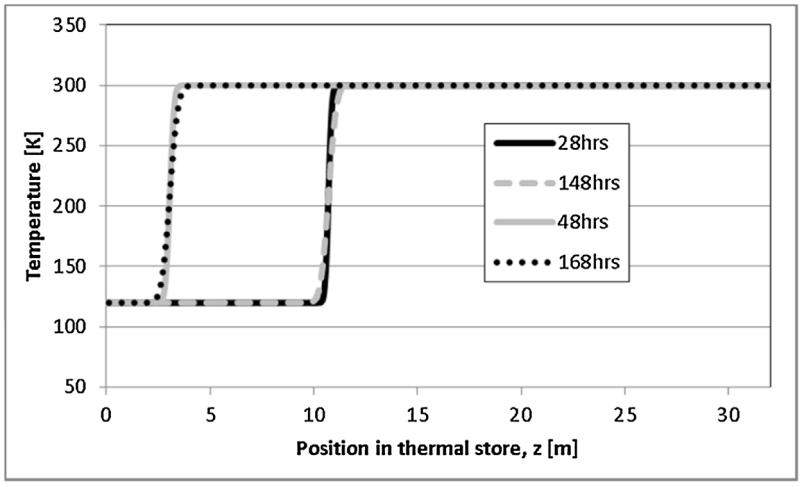

Fig. 21. Progression of thermal front in liquid thermocline store following charge discharge cycle shown in Table 1 with nominal 2 MW of heat being pumping out of the store during charging (5.84 kg/s of isopentane at 120 K).

considered. We use the Ergun equation as follows to calculate the pressure difference and then the required work to compress the gas [7] as a function of sphere radius i.e.

$$\frac{dP}{dx} = \frac{150\mu(1-\varepsilon)^2}{4R^2 \quad \varepsilon^3} v_s + \frac{1.75\rho_g(1-\varepsilon)}{2R \quad \varepsilon^3} v_s|v_s| \tag{45}$$

The pressure drop and associated exergy loss are calculated through-out the numerical simulation. Fig. 22 shows how the combination of irreversible heat transfer losses and work required to compress the gas result in a total exergy loss that depends on sphere size. Intuitively small spheres require greater pressure drop and gas compression work, however they also bring higher heat transfer area and so lower heat transfer losses. These two contradictory effects mean that an optimum sphere size can be found. For our example case this is found to be around a radius of 3 mm. Fig. 23 shows the total exergy loss that occurs after completion of the duty cycle as a function of the aspect ratio of the thermal store. The total store volume is kept constant and the length and radius varied to achieve the range of aspect ratios modelled. As aspect ratio is increased pressure drop increases due to the reduced flow area but heat transfer losses are reduced due to the higher velocities driving larger heat transfer coefficients. Using these simulation techniques an optimum aspect ratio can also be found and for our example this is around 3. This corresponds to a 32 m long 5 m radius store which is conveniently of similar size and geometry to the float of a large floating wind turbine platform.

Fig. 24 shows the exergy loss as a function of store aspect ratio for the laminar stratified isopentane store. In this case the exergy loss due to pumping the liquid is very small because the liquid is incompressible and so all that is required is a positive displacement pump to overcome friction in the circuit. As aspect ratio is reduced exergy loss increases due to thermal diffusion acting over an increasing cross sectional area. It should be noted that with an aspect ratio of 3 the exergy loss is 2.5 GJ as compared to 30 GJ for the packed bed. If we average the total loss over the duration of the example duty cycle it equates to 3.7 kW vs 44.3 kW for the packed bed.

The liquid thermocline model was based on a fully stratified laminar liquid. Turbulent diffusivities could easily be one or two orders of magnitude higher than the molecular thermal diffusivity assumed here depending on the scale and intensity of turbulence. Thus turbulence has the potential to significantly degrade the effectiveness of a liquid thermocline, and many complex studies of this have been carried out for example by Tinaikar et al. [4].

We believe that we can mitigate this problem and further reduce the exergy loss of a laminar stratified liquid thermocline by fitting an insulating sliding divider to separate the warm and cold sides of the thermal store (Fig. 25). As there is an appreciable

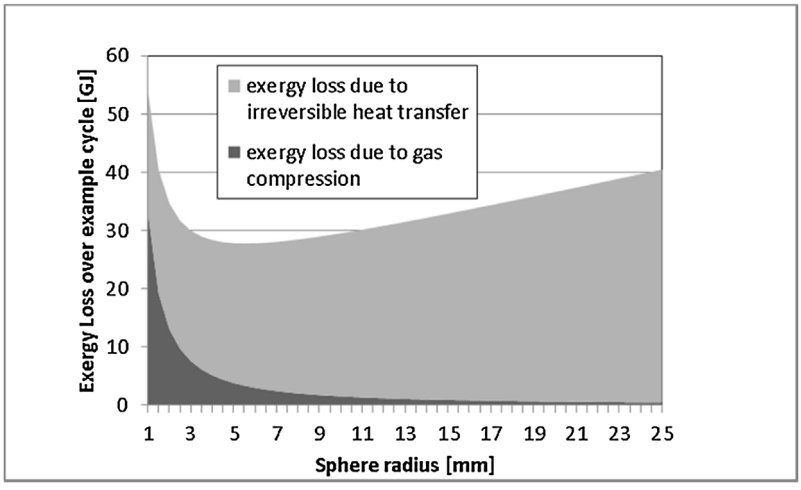

Fig. 22. Exergy loss in packed bed thermocline following example duty cycle as a function of sphere radius, (store aspect ratio = 3.2).

Please cite this article in press as: T.R. Davenne, et al., The cold store for a pumped thermal energy storage system, J. Energy Storage (2017), http://dx.doi.org/10.1016/j.est.2017.03.009

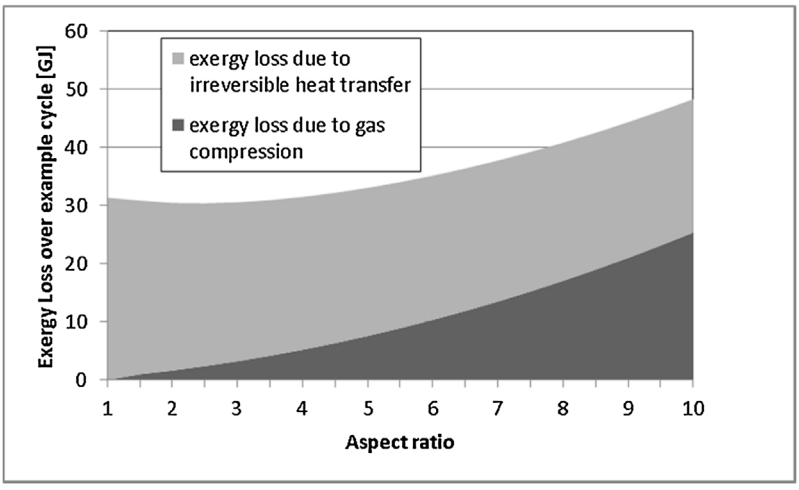

Fig. 23. Exergy loss in packed bed thermocline following example duty cycle as a function of thermal store aspect ratio (sphere radius = 3 mm).

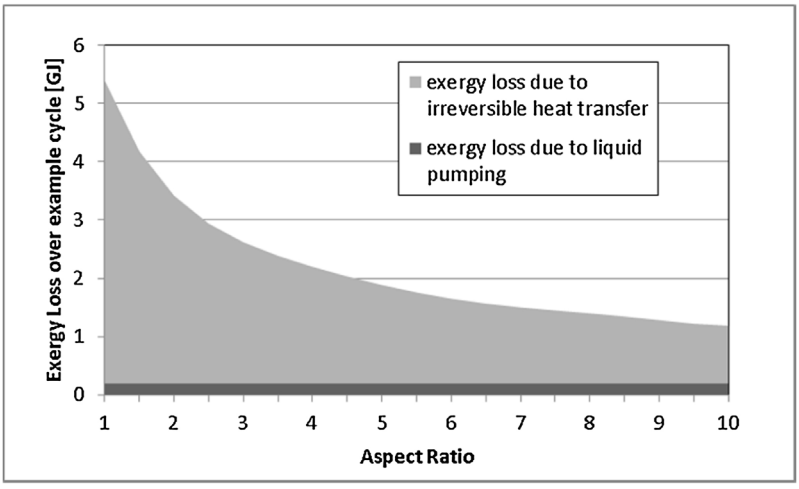

Fig. 24. Exergy loss in isopentane thermocline following example duty cycle as a function of thermal store aspect ratio.

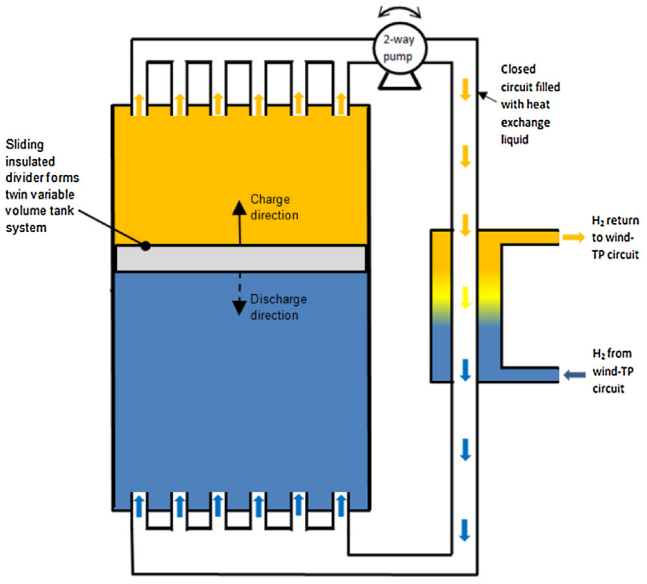

Fig. 25. Liquid cold store with sliding insulated divider forming two variable storage volumes.

density difference between the warm and cold fluid the divider could float on the denser cold fluid and it would be moved up and down as the thermal store is charged and discharged.

The primary function of the divider is to avoid the potential problem of thermocline instability caused by turbulence. The sliding divider would be designed as a thermal break so that negligible heat transfer was able to occur across it. The more conventional two tank system as described in Fig. 13 also solves the problem of irreversible heat transfer losses across a thermocline, however it requires double the total tank volume of this approach because half the total volume is always empty.

4. Conclusions

The hot and cold store of an ideal pumped thermal energy storage system require the same thermal mass.

Exergy loss by heat transfer from the periphery of the cold store is manageable to a reasonably low level (10 kW) with 1 m of insulation even with increased surface heat transfer rates that may be expected if the store is submerged under water.

Exergy loss when a thermal store is left idle is found to be similar for a packed bed and liquid thermocline.

One dimensional models of a stratified liquid and packed bed thermocline are presented. The analogous nature of thermocline

Please cite this article in press as: T.R. Davenne, et al., The cold store for a pumped thermal energy storage system, J. Energy Storage (2017), http://dx.doi.org/10.1016/j.est.2017.03.009

smearing due to thermal diffusion in a liquid and a packed bed thermocline is highlighted. An effective diffusivity parameter for a packed bed thermal store is presented. Its dependance on the parameters describing the packed bed is written explicitly. The stratified liquid thermocline is found to have significantly lower thermal diffusivity than the effective diffusivity of a packed bed giving it correspondingly lower heat transfer losses during charging and discharging.

Isopentane (used in geothermal plants) remains a liquid and maintains volumetric heat capacity across the entire operating temperature range of the Wind-TP cold store making it a candidate fluid for a liquid cold store.

Simulation of a the packed bed shows that exergy loss depends on sphere size and thermal store aspect ratio. Exergy loss was calculated following an example duty cycle and optimum sphere radii and aspect ratio were determined. The optimum radius and aspect ratio for the presented cold store example were 3 mm and 3 respectively. These preferred parameters yielded an average exergy loss rate of 44 kW over an example duty cycle.

Simulation of an isopentane liquid thermocline showed that exergy loss reduces with increasing aspect ratio. Exergy loss was calculated over the same example duty cycle and was found to be significantly lower than the packed bed at 3.7 kW.

In this example of a wind driven pumped thermal energy storage system a liquid thermocline cold store is predicted to result in a total exergy loss of the order of 14 kW (less than 1% of rated power) while a packed bed cold store will be of the order 55 kW (2.5% of rated power).

A sliding divider is proposed as a way of making a single tank liquid store into a twin variable volume tank with the same performance benefits as a conventional two tank system but without the extra volume requirement.

Appendix A. Semi Implicit method for solving Schumann's packed bed equations

Start by integrating Eq. (30) over a spatial step assuming T_s is constant across that step which gives the following

$$\left[ln(T_s - T_g)\right] = \left[-\frac{z}{l}\right]$$

Adding the limits as each side of the spatial step gives

$$T_{g_i}^{\ n} = T_s\left(1 - e^{-\frac{\Delta z}{l}}\right) + T_{g_{i-1}}^{\ n} e^{-\frac{\Delta z}{l}}$$

Then using the following

$$T_s = \frac{T_{s_{i-1}}^{\ n} + T_{s_i}^{\ n}}{2}$$

We get

$$T_{g_i}^{\ n} = T_{s_{i-1}}^{\ n}\left(1 - e^{-\frac{\Delta z}{l}}\right) + T_{s_i}^{\ n}\left(1 - e^{-\frac{\Delta z}{l}}\right) + T_{g_{i-1}}^{\ n} e^{-\frac{\Delta z}{l}}$$

Then integrate Eq. (31) over each time step assuming T_g is constant. Following the same procedure gives a similar expression for T_s and then writing the two expressions in matrix form gives the following

$$\begin{bmatrix} 1 & 0.5(a-1) \\ 0.5(b-1) & 1 \end{bmatrix} \begin{bmatrix} T_{g_i}^{\ n} \\ T_{s_i}^{\ n} \end{bmatrix} = \begin{bmatrix} T_{s_{i-1}}^{\ n}(1-a) + T_{g_i}^{\ n-1} a \\ T_{g_i}^{\ n-1}(1-b) + T_{s_{i-1}}^{\ n} b \end{bmatrix}$$

Where $a = e^{-\frac{\Delta z}{l}}$ and $b = e^{-\frac{\Delta t}{\tau}}$

Then invert the 2×2 matrix to find $\begin{bmatrix} T_{g_i}^{\ n} \\ T_{s_i}^{\ n} \end{bmatrix}$ which represents the gas and solid temperatures at the next step in time.

The computational space is represented with the following grid of points

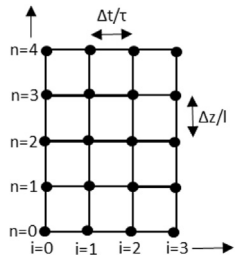

The initial condition for all values in space i.e. all values of n is applied to the left hand column of nodes (i = 0). The value at n = 0 remains a user input for all i as this corresponds to the inlet temperature to the store. Knowing the value of T_g and T_s at i = 1,n = 0 and i = 0, n = 1 then the value at i = 1, n = 1 can be found using the matrix inversion. After each column in space is completed the algorithm marches on to the next column corresponding to a step forward in time.

Appendix B. Explicit Method for solving Packed bed problem

Discretised equations for explicit 1D packed bed model

Consider energy balance in an elemental volume of gas

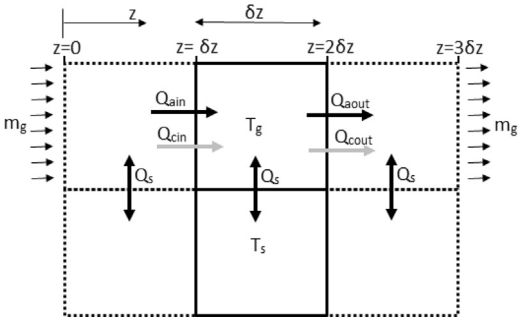

Rate of change of energy within gas = Net heat flow in by advection + Net heat flow in by conduction – Heat transferred to solid

This can be expressed as the following where i is the integer index for z and j is the index for time.

$$\rho_g C_{pg} A_s \delta z (T_g(i,j+1) - T_g(i,j)) = \frac{m_g C_{pg}}{2}(T_g(i-1,j) - T_g(i+1,j))\delta t + kA\left(\frac{T_g(i-1,j) - 2T_g(i,j) + T_g(i+1,j)}{\delta z}\right)\delta t - hA(T_g(i,j) - T_s(i,j))\delta t$$

Note that

$$Q_{ain} = m_g C_{pg}\left(\frac{T_g(i-1,j) + T_g(i,j)}{2}\right)\delta t$$

$$Q_{aout} = m_g C_{pg}\left(\frac{T_g(i+1,j) + T_g(i,j)}{2}\right)\delta t$$

and

$$Q_{cin} = kA\left(\frac{T_g(i-1,j) - T_g(i,j)}{\delta z}\right)\delta t$$

$$Q_{cout} = kA\left(\frac{T_g(\mathrm{i},\mathrm{j}) - T_g(\mathrm{i}+1,\mathrm{j})}{\delta z}\right)\delta t$$

Please cite this article in press as: T.R. Davenne, et al., The cold store for a pumped thermal energy storage system, J. Energy Storage (2017), http://dx.doi.org/10.1016/j.est.2017.03.009

Re-arranging for $T_g(i,j+1)$ gives

$$T_g(i,j+1) = T_g(i,j) + \frac{\left[\begin{array}{c}\frac{m_g C_{pg}}{2}(T_g(i-1,j) - T_g(i+1,j)) \\ +kA\left(\frac{T_g(i-1,j) - 2T_g(i,j) + T_g(i+1,j)}{\delta z}\right) - hA(T_g(i,j) - T_s(i,j))\end{array}\right]\delta t}{\rho_g C_{pg} A_s \delta z}$$

Then on each time step use the following to update solid temperature

$$T_s(i,j+1) = T_s(i,j) + \frac{hA}{\rho_s C_{ps} \varepsilon A_s \delta z}(T_g(i,j) - T_s(i,j))\delta t$$

This method can be implemented as a simple Euler method with a suitably small time step to ensure stability or a more advanced adaptive time step scheme can be employed where the time step is varied depending on the rate of change of temperature at any point in the simulation.

Appendix C. Explicit method for solving convection diffusion-equation to represent a liquid thermocline

Discretised equations for explicit 1D liquid thermocline

Consider energy balance in an elemental volume of liquid

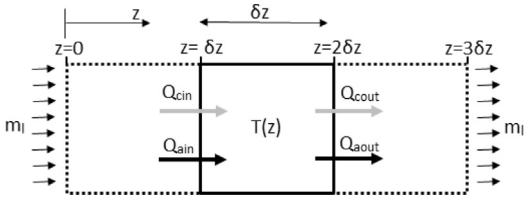

Rate of change of energy within gas = Net heat flow in by advection + Net heat flow in by conduction

This can be expressed as the following where i is the integer index for z and j is the index for time.

$$\rho_l C_{pl} A \delta z\left(T(i,j+1) - T(i,j)\right) = \frac{m_l C_{pl}}{2}(\mathrm{T}(i-1,j) - \mathrm{T}(i+1,j))\delta t + k_l A\left(\frac{T(i-1,j) - 2T(i,j) + T(i+1,j)}{\delta z}\right)\delta t$$

Note that

$$Q_{ain} = m_l C_{pl}\left(\frac{T(i-1,j) + T(i,j)}{2}\right)\delta t$$

$$Q_{aout} = m_l C_{pl}\left(\frac{T(i+1,j) + T(i,j)}{2}\right)\delta t$$

and

$$Q_{cin} = k_l A\left(\frac{T(\mathrm{i}-1,j) - T(i,j)}{\delta z}\right)\delta t$$

$$Q_{cout} = k_l A\left(\frac{T((i,j) - T(i+1,j)}{\delta z}\right)\delta t$$

Re-arranging for $T(i,j+1)$ gives

$$T(i,j+1) = T(i,j) + \frac{\left[\frac{m_g C_{pg}}{2}(T(i-1,j) - T(i+1,j)) + kA\left(\frac{T(i-1,j) - 2T(i,j) + T(i+1,j)}{\delta z}\right)\right]\delta t}{\rho_g C_{pg} A \delta z}$$

This method can be implemented as a simple Euler method with a suitably small time step to ensure stability or a more advanced adaptive time step scheme can be employed where the time step is varied depending on the rate of change of temperature at any point in the simulation.

References

[1] T. Desrues, J. Ruer, P. Marty, J.F. Fourmigué, A thermal energy storage process for large scale electric applications, J. Appl. Therm. Eng. 30 (April (5)) (2010) 425–432.
[2] Isentropic Ltd http://www.isentropic.co.uk/.
[3] S.D. Garvey, et al., Analysis of a wind turbine power transmission system with intrinsic energy storage capability, Wind Eng. 39 (2) (2015) 149–174.
[4] A. Tinaikar, S. Advaith, Spatio-temporal disruption of thermocline by successive laminar vortex pairs in a single tank thermal energy storage, Appl. Therm. Eng. (April) (2016).
[5] R.B. Kogbara, S.R. Iyengar, Z.C. Grasley, E.A. Masad, D.G. Zollinger, A review of concrete properties at cryogenic temperatures: towards direct LNG containment, J. Construction Building Mater. 47 (October) (2013) 760–770.
[6] C., Travis Anderson, The Heat Capacities of Quartz, Cristobalite and Tridymite at Low Temperatures, doi: 10.1021/ja01295a008.
[7] S. Ergun, Fluid flow through packed bed columns, J Chem. Process Eng. London (1952).
[8] A. Fick, On liquid diffusion, J. Membr. Sci. 100 (1995) 33–38 (reproduced from original 1855 paper).
[9] R.W. Garman, A CFD Assessment of Heat Transfer Through a Ship's Hull, Anteon Corporation, 2017.
[10] P.W. Dietz, Effective thermal conductivity of packed beds, J. Ind. Eng. Chem. Fundam. 18 (3) (1979).
[11] T. Schumann, Heat transfer: a liquid flowing through a porous prism, J. Franklin Inst. 208 (1929) 405–416.
[12] A.J. White, Loss analysis of thermal reservoirs for electrical energy storage schemes, Appl. Energy 88 (11) (2011) 4150–4159.
[13] A. Willmot, Dynamics of Regenerative Heat Transfer, Taylor & Francis, 2002.
[14] A. Cybulski, M.J. Van Dalen, J.W. Verkerk, P.J. Van Den Berg, Gas particle heat transfer coefficients in packed beds at low Reynolds number, J. Chem. Eng. Sci. 30 (1975) 1015–1018.
[15] A. White, J. McTigue, C. Markides, Wave propagation and thermodynamic losses in packed-bed thermal reservoirs for energy storage, J. Appl. Energy 130 (October) (2014) 648–657.

Please cite this article in press as: T.R. Davenne, et al., The cold store for a pumped thermal energy storage system, J. Energy Storage (2017), http://dx.doi.org/10.1016/j.est.2017.03.009